

01 Jan 1989

## N, L Distributions For Electron-Capture From H(1s) By C<sup>6+</sup> and O<sup>8+</sup>

Ronald E. Olson

Missouri University of Science and Technology, [olson@mst.edu](mailto:olson@mst.edu)

D. R. Schultz

Follow this and additional works at: [https://scholarsmine.mst.edu/phys\\_facwork](https://scholarsmine.mst.edu/phys_facwork)

 Part of the [Physics Commons](#)

---

### Recommended Citation

R. E. Olson and D. R. Schultz, "N, L Distributions For Electron-Capture From H(1s) By C<sup>6+</sup> and O<sup>8+</sup>," *Physica Scripta*, vol. 1989, no. T28, pp. 71 - 76, IOP Publishing; Royal Swedish Academy of Sciences, Jan 1989. The definitive version is available at <https://doi.org/10.1088/0031-8949/1989/T28/013>

This Article - Journal is brought to you for free and open access by Scholars' Mine. It has been accepted for inclusion in Physics Faculty Research & Creative Works by an authorized administrator of Scholars' Mine. This work is protected by U. S. Copyright Law. Unauthorized use including reproduction for redistribution requires the permission of the copyright holder. For more information, please contact [scholarsmine@mst.edu](mailto:scholarsmine@mst.edu).

## $n, l$ Distributions for Electron-Capture from H(1s) by $C^{6+}$ and $O^{8+}$

To cite this article: R E Olson and D R Schultz 1989 *Phys. Scr.* **1989** 71

View the [article online](#) for updates and enhancements.

### You may also like

- [Final-state-resolved charge exchange in  \$C^{6+}\$  collisions with H](#)  
J L Nolte, P C Stancil, H P Liebermann et al.
- [Scaling for state-selective charge exchange due to collisions of multicharged ions with hydrogen](#)  
A Jorge, Clara Illescas, J E Miraglia et al.
- [Charge transfer and ionization cross-sections in collisions of singly charged lithium ions with helium and nitrogen atoms](#)  
M Al-Ajaleen, A Taoutioui and K Tkési

# $n, l$ Distributions for Electron-Capture from $H(1s)$ by $C^{6+}$ and $O^{8+}$

R. E. Olson and D. R. Schultz

Department of Physics and Laboratory for Atomic Molecular Research, University of Missouri–Rolla, Rolla, Missouri 65401, U.S.A.

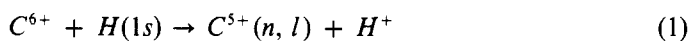
Received September 21, 1988; accepted October 16, 1988

## Abstract

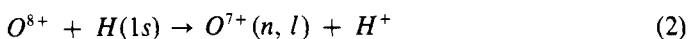
Total cross sections for electron-capture from the ground state of hydrogen by  $C^{6+}$  (40, 50, 60, 80, 100 and 120 keV/u) and  $O^{8+}$  (40, 50, 60, 80, 100, 120 and 140 keV/u) have been calculated using the classical-trajectory Monte Carlo (CTMC) technique. We tabulate these cross sections as a function of projectile energy for (i) capture to all product states, (ii) capture to product  $n$ -levels, and (iii) capture to product  $n, l$ -levels. The results of these calculations agree with and extend previous CTMC  $n, l$  distribution results [1].

## 1. Introduction

We consider here the charge transfer collisions



and



where the  $C^{6+}$  and  $O^{8+}$  ions range in energy from 40 to 140 keV/u. Detailed knowledge of the cross sections for these reactions is of great practical importance to tokamak fusion development because these processes play a large role in the energy loss mechanisms which compete with the heating of the plasma. Furthermore, knowledge of these cross sections is quite useful in providing fusion plasma diagnostics, especially in measurements of neutral beam penetration depths. Since it is the isotopes of hydrogen that are used in forming fusion plasmas, we note that the cross sections for reactions (1) and (2) are the same as those for processes involving deuterium and tritium at the same relative collision velocity and therefore, for simplicity, we present results only for ordinary hydrogen.

The dominant mechanisms which cause energy loss from the plasma are due to the presence of impurities. Residual neutral hydrogen molecules, which can escape the confining magnetic fields, create these impurities by sputtering occluded gases, such as oxygen and carbon monoxide, or other heavy ions, such as iron, from the torus walls. Once released, these species undergo collisions with the ions and electrons of the plasma, producing various charge states and levels of excitation of the impurity ions and thereby removing energy from the plasma by bremsstrahlung and line radiation.

Of particular importance for neutral beam heating, a technique to heat the plasma beyond the limitations of ohmic heating, are charge transfer collisions between the injected neutral deuterium beam and fully stripped carbon and oxygen. The probability of capture into the  $n = 4$  and 5 manifolds of  $C^{5+}$  and the  $n = 6, 7,$  and 8 manifolds of  $O^{7+}$  are enhanced due to the fact that the hydrogen ground state energy matches the energies of these levels. The distribution over a few  $n$ -levels arises due to the range of possible collision

dynamics. Subsequent line radiation from these excited states results in energy loss and impairment of the neutral beam heating efficiency. A useful side effect of these enhanced capture processes is that they provide information as to the depth of penetration of the neutral beam before ionization. Since other processes which lead to the capture of an electron by these fully stripped ions result principally in distributions lower in  $n$ -level, the line radiation signature of these reactions indicates the depth of neutral beam penetration.

Thus, knowledge of the measured plasma radiation spectrum as well as of the various cross sections for capture, allows the inference of the concentration and spatial distribution of impurities. It also provides important information for computer simulations of these atomic processes in fusion plasmas. Therefore, we present here cross sections for various product state distributions for reactions (1) and (2) calculated using the classical-trajectory Monte Carlo (CTMC) technique. Previous work [1] has described the dominant features of the product  $n, l$  distribution for charge transfer in multiply charged ion collisions with ground state hydrogen and surveyed the effects of the varying charge state of the projectile on these product distributions at 50 and 100 keV/u collision energies. The distributions tabulated here confirm the results of the previous calculations and extend them to a wider range of collision energies, specifically for the important reactions  $C^{6+} + H(1s)$  and  $O^{8+} + H(1s)$ .

## 2. Theoretical method

The CTMC method for ion-atom collisions has been described in detail by Percival and Richards [2], Olson and Salop [3], Olson [4] and in particular in its application to charge transfer to various  $n, l$ -levels, by Becker and MacKellar [5] and Olson [1]. Here we apply this method to ion-hydrogen collisions and thus employ a three-body (projectile, target nucleus and target electron) model which includes all two-body Coulomb interactions. The CTMC method is a technique in which a large ensemble of projectile-target configurations is sampled in order to simulate the collision process. The Monte Carlo nature of the method consists of choosing initial configurations of the target hydrogen atom, according to a model described by Abrines and Percival [6], whose ensemble properties reproduce the quantum mechanical orbital electron momentum distribution. The classical trajectories of the three bodies are then found by iteratively solving Hamilton's equations of motion. After the integration has been carried out into the asymptotic region, the relative energies of the particles is found to determine what, if any reaction has occurred.

In the event that the electron is captured by the projectile,

a product classical  $n$ -level is assigned according to

$$n_c = q/(2U)^{1/2} \quad (3)$$

where  $q$  is the charge of the incident ion and  $U$  is the product state binding energy. Here, and in the expressions which follow, we employ atomic units for convenience. Also, the classical orbital angular momentum of the captured electron is defined by

$$l_c = [(x\dot{y} - y\dot{x})^2 + (x\dot{z} - z\dot{x})^2 + (y\dot{z} - z\dot{y})^2]^{1/2}, \quad (4)$$

where  $x$ ,  $y$  and  $z$  are the Cartesian coordinates of the electron relative to the projectile nucleus after capture.

Becker and MacKeller [5] have used a principle of proportionality of classical and quantal weights in order to identify quantal product  $n, l$ -levels from the classical values determined by eqs. (3) and (4). By requiring that the phase space per bin be equal to the quantal  $n^2$  multiplicity of a given level  $n$ , they have shown that the relation

$$[(n-1)(n-\frac{1}{2})n]^{1/3} \leq n_c \leq [n(n+\frac{1}{2})(n+1)]^{1/3} \quad (5)$$

determines the correspondence between classical and quantal  $n$ -levels. Further, in the classical microcanonical ensemble,  $l_c^2$  is uniformly distributed for a given  $n$ -level. Thus, after normalizing the values of  $l_c$  by multiplying by  $n/n_c$  to reflect the fact that they correspond to noninteger classical  $n$ -levels, the correct quantal weight for a given  $l$ , namely  $2l+1$ , is reproduced if

$$l \leq l_c \leq l+1. \quad (6)$$

Therefore, relations (5) and (6) provide a prescription for determining the appropriate quantal product  $n, l$ -levels.

### 3. Results

In Table I we present CTMC total cross sections for capture to all product states for reactions (1) and (2) in the projectile energy range of 40–140 keV/u. These cross sections, as well as those in the subsequent tables, are given with two standard deviation error limits since the Monte Carlo method provides a statistical way to define the uncertainty. The statistical uncertainties in these total cross sections is about one percent, indicating that the probability for these processes is relatively high and that a very large number of classical trajectories were computed. In fact, the cross sections tabulated here represent the results of approximately two million Monte Carlo collisions. The large number of trials was required because these total cross sections have also been broken down into  $n$ -level and  $n, l$ -level cross sections, resulting in a smaller number of counts in a particular reaction sub-channel and therefore increasing the statistical uncertainty. The  $n, l$  cross sections summed over  $n$  and  $l$  thus provide a benchmark for comparison for other experimental and theoretical determinations.

Cross sections for capture by  $C^{6+}$  and  $O^{8+}$  to specific  $n$ -levels are tabulated in Tables II and III, respectively. The truncation of these tables at some large  $n$ -level reflects the fact that a certain point is reached beyond which insufficient Monte Carlo trials exist in a particular channel to report a cross section within reasonable error limits. Inspection of the tables indicates that in this energy regime, capture occurs predominantly to levels with principal quantum number around

$$n_m = q^{3/4} \quad (7)$$

where  $q$  is the projectile charge. This maximum in the  $n$  distribution occurs at about  $n = 4$  for  $C^{6+}$  and  $n = 5$  for  $O^{8+}$ . As observed in Ref. [1] this behavior implies that the captured electron preferentially preserves both its original energy and orbital dimensions after the charge transfer collision. As a function of increasing projectile energy, the  $n$ -level distributions broaden while the position of the maxima remain nearly constant.

In Tables IV and V we present the product state  $n, l$  distributions for reactions (1) and (2). The statistical uncertainties in these cross sections is larger than those for the  $n$ -level cross sections due to the fact that, as mentioned above, the number of Monte Carlo trials has been divided among a large number of subchannels. To illustrate the behavior of the  $n, l$  distributions we have included cross sections with rather large statistical uncertainties and, therefore, point out that caution should be used when interpreting the table entries for channels with very small cross sections. Processes with cross sections less than approximately  $10^{-20}$  cm<sup>2</sup> resulted in zero Monte Carlo events and thus calculated cross sections of zero. These zero values have been replaced with a dash mark in the tables to emphasize the fact that the calculated cross section is simply below the level required for sufficient statistics.

We may, however, draw several conclusions from these calculations since the bulk of the cross sections have reasonably small uncertainties. In fact, for  $n < n_m$  the orbital angular momentum quantum numbers are more highly peaked than statistical to large  $l$  values, while for  $n > n_m$  they maximize around  $l = q^{3/4}$ . This occurs because the low  $n$ -level populations arise primarily from small impact parameter collisions in which an electron with high orbital angular momentum is captured from a tight, nearly circular classical orbit. For larger  $n$ -levels, electrons with large classical eccentricities, and therefore low angular momenta, are preferentially captured in large impact parameter collisions. Thus, processes which preserve the electron's orbital angular momentum appear to be preferred.

### 4. Conclusion

The CTMC method has been used to calculate product  $n, l$  distributions for charge transfer collisions which play an important role in the atomic physics of tokamak fusion plasmas, that is  $C^{6+} + H(1s)$  and  $O^{8+} + H(1s)$ , for projectile energies between 40 and 140 keV/u. We confirm our previous results that the  $n$ -level distributions maximize at  $n_m \approx q^{3/4}$  and that the  $l$ -level distributions reflect the tendency of the captured electron to preserve its classical eccentricity and therefore its orbital angular momentum.

### Acknowledgement

The authors gratefully acknowledge the support of the Office of Fusion Research, United States Department of Energy.

### References

1. Olson, R. E., Phys. Rev. **A24**, 1726 (1981).
2. Percival, I. C. and Richards, D., Advances in Atomic and Molecular Physics, Vol. 11, 1 (1975).
3. Olson, R. E. and Salop, A., Phys. Rev. **A16**, 531 (1977).
4. Olson, R. E., Phys. Rev. **A27**, 1871 (1983).
5. Becker, R. L. and MacKellar, A. D., J. Phys. **B17**, 3923 (1984).
6. Abrines, R. and Percival, I. C., Proc. Phys. Soc. London **88**, 861 (1966).

Table I. Total cross sections for capture to all states from the ground state of hydrogen (given in units of 10<sup>-16</sup> cm<sup>2</sup> with two standard deviation error limits)

C <sup>6+</sup> + H			O <sup>8+</sup> + H		
<i>E</i> (keV/u)	$\sigma$	$\Delta\sigma$	<i>E</i> (keV/u)	$\sigma$	$\Delta\sigma$
40	25.7	(0.306)	40	36.2	(0.420)
50	24.3	(0.302)	50	34.3	(0.415)
60	21.6	(0.267)	60	32.0	(0.345)
80	14.4	(0.155)	80	23.9	(0.269)
100	8.88	(0.134)	100	16.0	(0.204)
120	5.35	(0.107)	120	10.0	(0.152)
			140	6.33	(0.108)

Table II. Total cross sections for capture from H(1s) by C<sup>6+</sup> to various *n*-levels (given in units of 10<sup>-16</sup> cm<sup>2</sup> with two standard deviation error limits)

<i>n</i>	40 keV/u		50 keV/u		60 keV/u	
	$\sigma$	$\Delta\sigma$	$\sigma$	$\Delta\sigma$	$\sigma$	$\Delta\sigma$
1	-	-	-	-	-	-
2	0.083	(0.022)	0.103	(0.024)	0.093	(0.021)
3	3.668	(0.141)	2.647	(0.121)	2.103	(0.098)
4	10.569	(0.227)	7.585	(0.197)	5.385	(0.154)
5	6.730	(0.186)	6.281	(0.181)	4.879	(0.147)
6	2.344	(0.114)	3.356	(0.135)	3.176	(0.120)
7	0.933	(0.072)	1.665	(0.096)	1.941	(0.095)
8	0.430	(0.049)	0.821	(0.068)	1.153	(0.073)
9	0.237	(0.037)	0.524	(0.054)	0.733	(0.059)
10	0.172	(0.031)	0.341	(0.044)	0.504	(0.049)
11	0.114	(0.025)	0.257	(0.038)	0.376	(0.042)
12	0.083	(0.022)	0.162	(0.030)	0.259	(0.035)
13	0.064	(0.019)	0.131	(0.027)	0.219	(0.032)
14	0.048	(0.017)	0.101	(0.024)	0.152	(0.027)
15	0.033	(0.014)	0.064	(0.019)	0.110	(0.023)

<i>n</i>	80 keV/u		100 keV/u		120 keV/u	
	$\sigma$	$\Delta\sigma$	$\sigma$	$\Delta\sigma$	$\sigma$	$\Delta\sigma$
1	-	-	0.001	(0.001)	0.001	(0.001)
2	0.113	(0.016)	0.099	(0.015)	0.092	(0.015)
3	1.454	(0.056)	0.909	(0.046)	0.578	(0.037)
4	2.881	(0.078)	1.566	(0.060)	0.893	(0.046)
5	2.708	(0.076)	1.498	(0.059)	0.842	(0.044)
6	1.984	(0.066)	1.165	(0.052)	0.674	(0.040)
7	1.329	(0.054)	0.837	(0.044)	0.477	(0.033)
8	0.944	(0.046)	0.634	(0.039)	0.376	(0.030)
9	0.679	(0.039)	0.441	(0.032)	0.294	(0.026)
10	0.438	(0.031)	0.349	(0.029)	0.203	(0.022)
11	0.400	(0.030)	0.260	(0.025)	0.171	(0.020)
12	0.301	(0.026)	0.222	(0.023)	0.144	(0.018)
13	0.215	(0.022)	0.167	(0.020)	0.118	(0.017)
14	0.178	(0.020)	0.117	(0.017)	0.083	(0.014)
15	0.140	(0.018)	0.118	(0.017)	0.071	(0.013)

Table III. Total cross sections for capture from H(1s) by C<sup>8+</sup> to various *n*-levels (given in units of 10<sup>-16</sup> cm<sup>2</sup> with two standard deviation error limits)

<i>n</i>	40 keV/u		50 keV/u		60 keV/u		80 keV/u	
	$\sigma$	$\Delta\sigma$	$\sigma$	$\Delta\sigma$	$\sigma$	$\Delta\sigma$	$\sigma$	$\Delta\sigma$
1	-	-	-	-	-	-	-	-
2	0.006	(0.007)	0.006	(0.007)	0.006	(0.006)	0.010	(0.006)
3	0.493	(0.062)	0.483	(0.061)	0.499	(0.054)	0.435	(0.043)
4	6.574	(0.218)	4.665	(0.186)	3.589	(0.142)	2.358	(0.098)
5	13.926	(0.304)	10.017	(0.264)	7.378	(0.199)	3.904	(0.125)
6	8.925	(0.251)	8.700	(0.248)	7.000	(0.194)	4.028	(0.127)
7	3.040	(0.151)	4.749	(0.187)	4.756	(0.162)	3.225	(0.114)
8	1.249	(0.098)	2.252	(0.131)	2.902	(0.128)	2.310	(0.097)
9	0.652	(0.071)	1.110	(0.092)	1.802	(0.102)	1.746	(0.085)
10	0.407	(0.056)	0.646	(0.071)	1.081	(0.079)	1.248	(0.072)
11	0.252	(0.044)	0.425	(0.057)	0.713	(0.064)	0.936	(0.063)
12	0.161	(0.035)	0.272	(0.046)	0.500	(0.054)	0.746	(0.056)
13	0.124	(0.031)	0.219	(0.041)	0.356	(0.046)	0.550	(0.048)
14	0.095	(0.027)	0.124	(0.031)	0.274	(0.040)	0.447	(0.043)
15	0.054	(0.021)	0.101	(0.028)	0.208	(0.035)	0.357	(0.039)
16	0.056	(0.021)	0.089	(0.026)	0.142	(0.029)	0.258	(0.033)
17	0.045	(0.019)	0.111	(0.029)	0.138	(0.028)	0.220	(0.030)
18	0.041	(0.018)	0.068	(0.023)	0.123	(0.027)	0.192	(0.028)
19	0.035	(0.016)	0.050	(0.020)	0.107	(0.025)	0.169	(0.027)
20	0.029	(0.015)	0.031	(0.016)	0.048	(0.017)	0.121	(0.023)

<i>n</i>	100 keV/u		120 keV/u		140 keV/u	
	$\sigma$	$\Delta\sigma$	$\sigma$	$\Delta\sigma$	$\sigma$	$\Delta\sigma$
1	-	-	-	-	-	-
2	0.016	(0.007)	0.017	(0.007)	0.015	(0.005)
3	0.307	(0.032)	0.274	(0.027)	0.229	(0.022)
4	1.377	(0.066)	0.889	(0.048)	0.635	(0.036)
5	2.197	(0.083)	1.325	(0.059)	0.856	(0.041)
6	2.308	(0.085)	1.326	(0.059)	0.812	(0.040)
7	1.975	(0.079)	1.194	(0.056)	0.710	(0.038)
8	1.561	(0.070)	0.943	(0.050)	0.585	(0.034)
9	1.264	(0.064)	0.718	(0.043)	0.451	(0.030)
10	0.983	(0.056)	0.595	(0.040)	0.357	(0.027)
11	0.731	(0.048)	0.480	(0.036)	0.275	(0.024)
12	0.555	(0.042)	0.395	(0.032)	0.217	(0.021)
13	0.448	(0.038)	0.300	(0.028)	0.205	(0.020)
14	0.387	(0.035)	0.259	(0.026)	0.164	(0.018)
15	0.281	(0.030)	0.221	(0.024)	0.121	(0.016)
16	0.243	(0.028)	0.191	(0.022)	0.106	(0.015)
17	0.236	(0.028)	0.151	(0.020)	0.095	(0.014)
18	0.216	(0.026)	0.125	(0.018)	0.084	(0.013)
19	0.168	(0.023)	0.098	(0.016)	0.063	(0.011)
20	0.136	(0.021)	0.089	(0.015)	0.055	(0.011)

Table IV. Total cross sections for capture from  $H(1s)$  by  $C^{6+}$  to various  $n, l$ -levels, (given in units of  $10^{-16} \text{ cm}^2$  with two standard deviation error limits)

40 keV/u									80 keV/u								
$n$	$l = 0$	1	2	3	4	5	6	7	$n$	$l = 0$	1	2	3	4	5	6	7
1	-								1	-							
2	0.020 (0.011)	0.063 (0.019)							2	0.030 (0.008)	0.083 (0.014)						
3	0.197 (0.033)	1.146 (0.080)	2.326 (0.113)						3	0.046 (0.010)	0.343 (0.028)	1.065 (0.049)					
4	0.100 (0.024)	0.825 (0.068)	2.835 (0.125)	6.809 (0.187)					4	0.044 (0.010)	0.246 (0.023)	0.642 (0.038)	1.949 (0.065)				
5	0.066 (0.019)	0.510 (0.054)	1.132 (0.080)	1.857 (0.102)	3.165 (0.131)				5	0.034 (0.009)	0.171 (0.020)	0.434 (0.031)	0.866 (0.044)	1.203 (0.051)			
6	0.026 (0.012)	0.181 (0.032)	0.359 (0.045)	0.563 (0.056)	0.874 (0.070)	0.342 (0.044)			6	0.022 (0.007)	0.142 (0.018)	0.267 (0.024)	0.524 (0.034)	0.741 (0.041)	0.288 (0.025)		
7	0.014 (0.009)	0.043 (0.016)	0.143 (0.028)	0.288 (0.040)	0.328 (0.043)	0.118 (0.026)	-	-	7	0.013 (0.005)	0.085 (0.014)	0.180 (0.020)	0.319 (0.027)	0.452 (0.032)	0.281 (0.025)	-	-
8	0.009 (0.007)	0.041 (0.015)	0.086 (0.022)	0.130 (0.027)	0.130 (0.027)	0.034 (0.014)	0.001 (0.003)	-	8	0.010 (0.005)	0.064 (0.012)	0.123 (0.017)	0.254 (0.024)	0.276 (0.025)	0.211 (0.022)	0.006 (0.004)	-
9	0.010 (0.008)	0.014 (0.009)	0.060 (0.018)	0.068 (0.020)	0.068 (0.020)	0.016 (0.009)	-	-	9	0.007 (0.004)	0.041 (0.010)	0.100 (0.015)	0.169 (0.019)	0.227 (0.023)	0.130 (0.017)	0.005 (0.003)	-
50 keV/u									100 keV/u								
$n$	$l = 0$	1	2	3	4	5	6	7	$n$	$l = 0$	1	2	3	4	5	6	7
1	-								1	0.001 (0.001)							
2	0.017 (0.010)	0.086 (0.022)							2	0.025 (0.008)	0.073 (0.013)						
3	0.125 (0.027)	0.762 (0.066)	1.759 (0.099)						3	0.028 (0.008)	0.209 (0.022)	0.672 (0.040)					
4	0.066 (0.019)	0.626 (0.059)	1.783 (0.100)	5.111 (0.164)					4	0.018 (0.007)	0.133 (0.018)	0.385 (0.030)	1.030 (0.049)				
5	0.073 (0.020)	0.428 (0.049)	1.009 (0.075)	1.733 (0.098)	3.038 (0.129)				5	0.020 (0.007)	0.105 (0.016)	0.250 (0.024)	0.522 (0.035)	0.601 (0.038)			
6	0.040 (0.015)	0.251 (0.038)	0.533 (0.055)	0.834 (0.069)	0.199 (0.082)	0.500 (0.053)			6	0.011 (0.005)	0.070 (0.013)	0.172 (0.020)	0.312 (0.027)	0.464 (0.033)	0.135 (0.018)		
7	0.024 (0.012)	0.145 (0.029)	0.284 (0.040)	0.398 (0.047)	0.552 (0.056)	0.262 (0.039)	-	-	7	0.010 (0.005)	0.045 (0.010)	0.109 (0.016)	0.236 (0.024)	0.303 (0.027)	0.133 (0.018)	0.001 (0.001)	
8	0.007 (0.006)	0.073 (0.020)	0.144 (0.029)	0.208 (0.034)	0.292 (0.041)	0.091 (0.023)	0.006 (0.006)	-	8	0.002 (0.002)	0.034 (0.009)	0.082 (0.014)	0.163 (0.020)	0.223 (0.023)	0.129 (0.017)	0.001 (0.001)	-
9	0.009 (0.007)	0.036 (0.014)	0.080 (0.021)	0.177 (0.032)	0.181 (0.032)	0.043 (0.016)	-	-	9	0.004 (0.003)	0.030 (0.008)	0.057 (0.012)	0.106 (0.016)	0.144 (0.018)	0.099 (0.015)	0.002 (0.002)	-
60 keV/u									120 keV/u								
$n$	$l = 0$	1	2	3	4	5	6	7	$n$	$l = 0$	1	2	3	4	5	6	7
1	-								1	0.001 (0.001)							
2	0.029 (0.012)	0.064 (0.017)							2	0.018 (0.006)	0.074 (0.013)						
3	0.090 (0.021)	0.536 (0.050)	1.477 (0.083)						3	0.013 (0.006)	0.124 (0.017)	0.441 (0.032)					
4	0.083 (0.020)	0.430 (0.045)	1.354 (0.079)	3.518 (0.126)					4	0.021 (0.007)	0.087 (0.014)	0.231 (0.023)	0.554 (0.036)				
5	0.052 (0.016)	0.300 (0.038)	0.735 (0.059)	1.474 (0.083)	2.317 (0.103)				5	0.009 (0.005)	0.068 (0.013)	0.157 (0.019)	0.300 (0.027)	0.308 (0.027)			
6	0.037 (0.013)	0.190 (0.030)	0.492 (0.048)	0.818 (0.062)	1.138 (0.073)	0.501 (0.049)			6	0.008 (0.004)	0.043 (0.010)	0.113 (0.016)	0.208 (0.022)	0.245 (0.024)	0.057 (0.012)		
7	0.018 (0.009)	0.148 (0.027)	0.285 (0.037)	0.424 (0.045)	0.685 (0.057)	0.379 (0.042)	0.001 (0.002)		7	0.005 (0.004)	0.033 (0.009)	0.073 (0.013)	0.136 (0.018)	0.161 (0.019)	0.068 (0.013)	-	-
8	0.014 (0.008)	0.088 (0.020)	0.156 (0.027)	0.280 (0.036)	0.382 (0.043)	0.230 (0.033)	0.002 (0.003)	-	8	0.004 (0.003)	0.026 (0.008)	0.049 (0.011)	0.103 (0.016)	0.124 (0.017)	0.071 (0.013)	-	-
9	0.005 (0.005)	0.062 (0.017)	0.120 (0.024)	0.176 (0.029)	0.243 (0.034)	0.124 (0.024)	0.004 (0.004)	-	9	0.004 (0.003)	0.018 (0.007)	0.043 (0.010)	0.079 (0.014)	0.100 (0.015)	0.049 (0.011)	0.001 (0.001)	-

Table V. Total cross sections for capture from H(1s) by O<sup>8+</sup> to various n, l-levels, (given in units of 10<sup>-16</sup> cm<sup>2</sup> with two standard deviation error limits)

40 keV/u									60 keV/u										
n	l = 0	1	2	3	4	5	6	7	8	n	l = 0	1	2	3	4	5	6	7	8
1	-									1	-								
	-										-								
2	0.002	0.004								2	0.003	0.003							
	(0.004)	(0.005)									(0.004)	(0.004)							
3	0.072	0.157	0.264							3	0.056	0.199	0.243						
	(0.024)	(0.035)	(0.045)								(0.018)	(0.034)	(0.038)						
4	0.165	0.914	2.465	3.030						4	0.085	0.411	1.139	1.954					
	(0.036)	(0.084)	(0.137)	(0.151)							(0.022)	(0.049)	(0.081)	(0.106)					
5	0.085	0.619	1.897	3.746	7.579					5	0.073	0.309	0.883	1.828	4.284				
	(0.026)	(0.069)	(0.120)	(0.167)	(0.233)						(0.021)	(0.043)	(0.072)	(0.102)	(0.155)				
6	0.016	0.283	0.852	1.274	2.128	4.372				6	0.037	0.232	0.597	1.022	1.735	3.378			
	(0.011)	(0.047)	(0.081)	(0.099)	(0.127)	(0.180)					(0.015)	(0.037)	(0.059)	(0.077)	(0.100)	(0.138)			
7	0.008	0.045	0.147	0.287	0.545	1.106	0.902			7	0.031	0.169	0.381	0.619	0.875	1.466	1.215		
	(0.008)	(0.019)	(0.034)	(0.047)	(0.065)	(0.092)	(0.083)				(0.013)	(0.031)	(0.047)	(0.060)	(0.071)	(0.092)	(0.084)		
8	0.012	0.021	0.058	0.173	0.231	0.380	0.359	0.016	-	8	0.016	0.109	0.202	0.327	0.504	0.831	0.809	0.103	-
	(0.010)	(0.013)	(0.021)	(0.037)	(0.042)	(0.054)	(0.053)	(0.011)	-		(0.010)	(0.025)	(0.034)	(0.044)	(0.054)	(0.069)	(0.069)	(0.025)	-
9	0.012	0.008	0.050	0.078	0.165	0.202	0.132	0.006	-	9	0.009	0.063	0.135	0.189	0.279	0.506	0.525	0.097	-
	(0.010)	(0.008)	(0.020)	(0.025)	(0.036)	(0.040)	(0.032)	(0.007)	-		(0.007)	(0.019)	(0.028)	(0.033)	(0.040)	(0.054)	(0.055)	(0.024)	-
10	0.004	0.016	0.035	0.068	0.103	0.116	0.052	0.014	-	10	0.001	0.037	0.079	0.122	0.174	0.295	0.304	0.069	-
	(0.005)	(0.011)	(0.016)	(0.023)	(0.028)	(0.030)	(0.020)	(0.010)	-		(0.003)	(0.015)	(0.022)	(0.027)	(0.032)	(0.042)	(0.042)	(0.020)	-
11	0.004	0.004	0.019	0.048	0.062	0.078	0.031	0.004	0.002	11	0.003	0.029	0.031	0.057	0.132	0.202	0.205	0.053	-
	(0.005)	(0.005)	(0.012)	(0.019)	(0.022)	(0.025)	(0.016)	(0.005)	(0.004)		(0.004)	(0.013)	(0.013)	(0.018)	(0.028)	(0.034)	(0.035)	(0.018)	-
12	-	0.012	0.019	0.033	0.037	0.035	0.023	0.002	-	12	0.004	0.015	0.009	0.056	0.101	0.142	0.150	0.023	-
	-	(0.010)	(0.012)	(0.016)	(0.017)	(0.016)	(0.013)	(0.004)	-		(0.005)	(0.009)	(0.007)	(0.018)	(0.024)	(0.029)	(0.030)	(0.012)	-

50 keV/u									80 keV/u										
n	l = 0	1	2	3	4	5	6	7	8	n	l = 0	1	2	3	4	5	6	7	8
1	-									1	-								
	-										-								
2	-	0.006								2	0.004	0.005							
	-	(0.007)									(0.004)	(0.005)							
3	0.064	0.169	0.250							3	0.025	0.168	0.242						
	(0.022)	(0.036)	(0.044)								(0.010)	(0.027)	(0.032)						
4	0.076	0.601	1.664	2.324						4	0.041	0.218	0.635	1.465					
	(0.024)	(0.068)	(0.113)	(0.133)							(0.013)	(0.030)	(0.052)	(0.078)					
5	0.081	0.469	1.193	2.485	5.788					5	0.040	0.175	0.459	0.923	2.307				
	(0.025)	(0.060)	(0.096)	(0.137)	(0.206)						(0.013)	(0.027)	(0.044)	(0.062)	(0.097)				
6	0.056	0.330	0.844	1.249	2.070	4.151				6	0.023	0.143	0.314	0.587	1.072	1.889			
	(0.021)	(0.050)	(0.081)	(0.098)	(0.125)	(0.176)					(0.010)	(0.025)	(0.036)	(0.050)	(0.067)	(0.088)			
7	0.025	0.198	0.415	0.576	0.871	1.451	1.212			7	0.021	0.097	0.226	0.433	0.672	1.022	0.754		
	(0.014)	(0.039)	(0.057)	(0.067)	(0.082)	(0.105)	(0.096)				(0.009)	(0.020)	(0.031)	(0.043)	(0.053)	(0.065)	(0.056)		
8	0.004	0.074	0.130	0.252	0.440	0.689	0.630	0.033	-	8	0.010	0.078	0.157	0.258	0.449	0.677	0.623	0.058	-
	(0.005)	(0.024)	(0.032)	(0.044)	(0.058)	(0.073)	(0.070)	(0.016)	-		(0.006)	(0.018)	(0.026)	(0.033)	(0.043)	(0.053)	(0.051)	(0.016)	-
9	0.006	0.027	0.078	0.132	0.200	0.345	0.297	0.025	-	9	0.012	0.064	0.135	0.191	0.293	0.491	0.468	0.092	-
	(0.007)	(0.015)	(0.025)	(0.032)	(0.039)	(0.052)	(0.048)	(0.014)	-		(0.007)	(0.016)	(0.024)	(0.028)	(0.035)	(0.045)	(0.044)	(0.020)	-
10	0.002	0.017	0.045	0.087	0.126	0.206	0.140	0.023	-	10	0.011	0.046	0.103	0.150	0.245	0.288	0.327	0.077	-
	(0.004)	(0.012)	(0.019)	(0.026)	(0.031)	(0.040)	(0.033)	(0.013)	-		(0.007)	(0.014)	(0.021)	(0.025)	(0.032)	(0.035)	(0.037)	(0.018)	-
11	0.002	0.010	0.035	0.060	0.118	0.109	0.085	0.006	-	11	0.002	0.030	0.076	0.131	0.140	0.231	0.247	0.078	-
	(0.004)	(0.009)	(0.016)	(0.022)	(0.030)	(0.029)	(0.026)	(0.007)	-		(0.003)	(0.011)	(0.018)	(0.024)	(0.024)	(0.031)	(0.032)	(0.018)	-
12	-	0.019	0.021	0.047	0.076	0.080	0.023	0.006	-	12	0.006	0.033	0.060	0.081	0.136	0.189	0.183	0.057	-
	-	(0.012)	(0.013)	(0.019)	(0.024)	(0.025)	(0.013)	(0.007)	-		(0.005)	(0.012)	(0.016)	(0.019)	(0.024)	(0.028)	(0.028)	(0.016)	-

*Table V. Continued*

100 keV/u									
<i>n</i>	<i>l</i> = 0	1	2	3	4	5	6	7	8
1	-								
2	0.002	0.014							
	(0.003)	(0.007)							
3	0.011	0.122	0.174						
	(0.006)	(0.020)	(0.024)						
4	0.019	0.111	0.353	0.894					
	(0.008)	(0.019)	(0.034)	(0.054)					
5	0.017	0.107	0.245	0.525	1.304				
	(0.007)	(0.019)	(0.028)	(0.041)	(0.064)				
6	0.011	0.086	0.195	0.364	0.689	0.963			
	(0.006)	(0.017)	(0.025)	(0.034)	(0.047)	(0.056)			
7	0.004	0.059	0.145	0.257	0.434	0.669	0.407		
	(0.004)	(0.014)	(0.022)	(0.029)	(0.037)	(0.046)	(0.036)		
8	0.014	0.049	0.104	0.181	0.289	0.482	0.411	0.031	-
	(0.007)	(0.013)	(0.018)	(0.024)	(0.031)	(0.039)	(0.036)	(0.010)	-
9	0.009	0.045	0.088	0.157	0.230	0.336	0.326	0.073	-
	(0.005)	(0.12)	(0.017)	(0.023)	(0.027)	(0.033)	(0.032)	(0.015)	-
10	0.003	0.022	0.045	0.105	0.191	0.261	0.281	0.076	-
	(0.003)	(0.008)	(0.012)	(0.018)	(0.025)	(0.029)	(0.030)	(0.016)	-
11	0.006	0.019	0.049	0.081	0.126	0.191	0.188	0.071	-
	(0.004)	(0.008)	(0.013)	(0.016)	(0.020)	(0.025)	(0.025)	(0.015)	-
12	0.004	0.017	0.036	0.062	0.091	0.144	0.146	0.055	-
	(0.004)	(0.007)	(0.011)	(0.014)	(0.017)	(0.022)	(0.022)	(0.013)	-

120 keV/u									
<i>n</i>	<i>l</i> = 0	1	2	3	4	5	6	7	8
1	-								
2	0.005	0.012							
	(0.004)	(0.006)							
3	0.013	0.089	0.172						
	(0.006)	(0.015)	(0.021)						
4	0.014	0.082	0.216	0.578					
	(0.006)	(0.015)	(0.024)	(0.039)					
5	0.015	0.075	0.161	0.303	0.771				
	(0.006)	(0.014)	(0.021)	(0.028)	(0.045)				

*Table V. Continued*

6	0.009	0.047	0.128	0.212	0.417	0.513			
	(0.005)	(0.011)	(0.018)	(0.024)	(0.033)	(0.037)			
7	0.009	0.035	0.086	0.167	0.283	0.421	0.193		
	(0.005)	(0.010)	(0.015)	(0.021)	(0.027)	(0.033)	(0.023)		
8	0.008	0.027	0.064	0.134	0.220	0.271	0.210	0.009	-
	(0.005)	(0.008)	(0.013)	(0.019)	(0.024)	(0.027)	(0.024)	(0.005)	-
9	0.007	0.026	0.046	0.080	0.163	0.188	0.184	0.024	-
	(0.004)	(0.008)	(0.011)	(0.015)	(0.021)	(0.022)	(0.022)	(0.008)	-
10	0.003	0.017	0.037	0.083	0.131	0.159	0.127	0.037	-
	(0.003)	(0.007)	(0.010)	(0.015)	(0.019)	(0.021)	(0.018)	(0.010)	-
11	0.001	0.016	0.036	0.048	0.101	0.116	0.122	0.040	-
	(0.002)	(0.006)	(0.010)	(0.011)	(0.016)	(0.017)	(0.018)	(0.010)	-
12	0.002	0.010	0.027	0.040	0.077	0.104	0.100	0.035	-
	(0.002)	(0.005)	(0.008)	(0.010)	(0.014)	(0.017)	(0.016)	(0.010)	-

140 keV/u									
<i>n</i>	<i>l</i> = 0	1	2	3	4	5	6	7	8
1	-								
2	0.004	0.011							
	(0.003)	(0.005)							
3	0.009	0.066	0.154						
	(0.004)	(0.012)	(0.018)						
4	0.009	0.055	0.133	0.438					
	(0.004)	(0.011)	(0.016)	(0.030)					
5	0.008	0.038	0.108	0.234	0.468				
	(0.004)	(0.009)	(0.015)	(0.022)	(0.031)				
6	0.007	0.032	0.081	0.143	0.244	0.305			
	(0.004)	(0.008)	(0.013)	(0.017)	(0.022)	(0.025)			
7	0.006	0.025	0.053	0.108	0.203	0.236	0.078		
	(0.003)	(0.007)	(0.010)	(0.015)	(0.020)	(0.022)	(0.013)		
8	0.005	0.022	0.043	0.082	0.133	0.176	0.121	0.003	-
	(0.003)	(0.007)	(0.009)	(0.013)	(0.016)	(0.019)	(0.016)	(0.002)	-
9	0.002	0.015	0.036	0.056	0.094	0.132	0.108	0.009	-
	(0.002)	(0.005)	(0.009)	(0.011)	(0.014)	(0.016)	(0.015)	(0.004)	-
10	0.001	0.008	0.025	0.050	0.072	0.100	0.093	0.009	-
	(0.001)	(0.004)	(0.007)	(0.010)	(0.012)	(0.014)	(0.014)	(0.004)	-
11	0.002	0.009	0.019	0.033	0.053	0.077	0.068	0.014	-
	(0.002)	(0.004)	(0.006)	(0.008)	(0.010)	(0.013)	(0.012)	(0.005)	-
12	0.002	0.007	0.013	0.035	0.043	0.053	0.052	0.013	-
	(0.002)	(0.004)	(0.005)	(0.008)	(0.009)	(0.010)	(0.010)	(0.005)	-